Light stress in green and red Planktothrix strains: The orange carotenoid protein and its related photoprotective mechanism

Chakib Djediat, Kathleen Feilke, Arthur Brochard, Lucie Caramelle, Sandra Kim Tiam, Pierre Sétif, Theo Gauvrit, Claude Yéprémian, Adjélé Wilson, Léa Talbot, et al.

Light stress in green and red Planktothrix strains: The orange carotenoid protein and its related photoprotective mechanism

Chakib Djediat, Kathleen Feilke, Arthur Brochard, Lucie Caramelle, Sandra Tiam, Pierre Sétif, Theo Gauvrit, Claude Yéprémian, Adjélé Wilson, Léa Talbot, et al.

BBA - Bioenergetics xxx (xxxx) xxx–xxx

Light stress in green and red *Planktothrix* strains: The orange carotenoid protein and its related photoprotective mechanism

Chakib Djediat[a,b,1], Kathleen Feilke[c,1], Arthur Brochard[a,b], Lucie Caramelle[a,b], Sandra Kim Tiam[b], Pierre Sétif[c], Theo Gauvrit[b], Claude Yéprémian[b], Adjélé Wilson[c], Léa Talbot[c], Benjamin Marie[b], Diana Kirilovsky[c,*], Cécile Bernard[b,**]

[a] *Electron Microscopy Platform, Muséum National d'Histoire Naturelle, CP 39, 12 rue Buffon, F-75231 Paris Cedex 05, France*
[b] *UMR 7245 MCAM, Muséum National d'Histoire Naturelle - CNRS, Paris, 12 rue Buffon, CP 39, 75231 Paris Cedex 05, France*
[c] *Institute for Integrative Biology of the Cell (I2BC), CNRS, Commissariat à l'Energie Atomique et aux Energies Alternatives, Université Paris-Sud, Université Paris-Saclay, 91198 Gif sur Yvette, France*

ARTICLE INFO

Keywords:
Cyanobacteria
Planktothrix
Orange carotenoid protein
Microcystin
Fluorescence

ABSTRACT

Photosynthetic organisms need to sense and respond to fluctuating environmental conditions, to perform efficient photosynthesis and avoid the formation of harmful reactive oxygen species. Cyanobacteria have developed a photoprotective mechanism that decreases the energy arriving at the reaction centers by increasing thermal energy dissipation at the level of the phycobilisome, the extramembranal light-harvesting antenna. This mechanism is triggered by the photoactive orange carotenoid protein (OCP). In this study, we characterized OCP and the related photoprotective mechanism in non-stressed and light-stressed cells of three different strains of *Planktothrix* that can form impressive blooms. In addition to changing lake ecosystemic functions and biodiversity, *Planktothrix* blooms can have adverse effects on human and animal health as they produce toxins (e.g., microcystins). Three *Planktothrix* strains were selected: two green strains, PCC 10110 (microcystin producer) and PCC 7805 (non-microcystin producer), and one red strain, PCC 7821. The green strains colonize shallow lakes with higher light intensities while red strains proliferate in deep lakes. Our study allowed us to conclude that there is a correlation between the ecological niche in which these strains proliferate and the rates of induction and recovery of OCP-related photoprotection. However, differences in the resistance to prolonged high-light stress were correlated to a better replacement of damaged D1 protein and not to differences in OCP photoprotection. Finally, microcystins do not seem to be involved in photoprotection as was previously suggested.

1. Introduction

Photosynthetic organisms have to cope with the impossibility to control incoming flux of light. Indeed while light is essential for photosynthetic organisms, full sunlight is harmful for them. Therefore, they have developed several photoprotective mechanisms to protect themselves from excess light. One mechanism involves the reduction of excitation energy funneled from the antenna into the photochemical centers (for a review see [1]). This decreases the accumulation of high-energy reactive oxygen species (ROS; singlet oxygen and oxygen radicals) generated during secondary reactions that occur when the photosynthetic electron transport chain is over-reduced. In cyanobacteria, the orange carotenoid protein (OCP), by interacting with the cyanobacterial antenna, the phycobilisome (PBS), induces thermal dissipation of the excess energy absorbed at the level of the PBS [2–4].

OCP is a photoactive soluble protein formed by two globular domains, the α helix N-terminal domain (NTD) and α-helix/β-sheet C-terminal domain (CTD) [5]. A ketocarotenoid, 3′ hydroxyechinenone, is shared by the two domains and is essential for OCP photoactivation [5–7]. Two other ketocarotenoids, echinenone and canthaxanthin, are able to bind to the OCP and to allow photoactivation [6,8]. The carbonyl group of the carotenoid is hydrogen-bound to Tyr201 and Trp288 in the CTD [5]. Upon illumination with strong blue light, OCP photoconverts from an orange closed inactive form (OCP^O) to a red open

* Correspondence to: D. Kirilovsky, Institute for Integrative Biology of the Cell (I2BC), CEA, CNRS, Université Paris-Sud, Université Paris-Saclay, 91198 Gif sur Yvette, France.
** Correspondence to: C. Bernard, UMR 7245 MCAM, Muséum National d'Histoire Naturelle - CNRS, Paris, 12 rue Buffon, CP 39, 75231 Paris Cedex 05, France.
E-mail addresses: diana.kirilovsky@cea.fr (D. Kirilovsky), cecile.bernard@mnhn.fr (C. Bernard).
[1] These authors contributed equally to this work.

Please cite this article as: Chakib Djediat, et al., BBA - Bioenergetics, https://doi.org/10.1016/j.bbabio.2019.06.009

active form (OCP^R) [7]. Upon light absorption by the carotenoid, the H bonds between the carotenoid and protein are broken, and the carotenoid translocates into the NTD by undergoing several intermediary steps [9–11]. Then, the interactions between the domains are disrupted, and the domains separate from each other [10,12]. Only OCP^R is able to interact with PBS [7,13]. The NTD of OCP^R binds to the core of the PBS and induces thermal dissipation of excess absorbed energy [13,14]. The two forms of the OCP are also efficient quenchers of singlet oxygen [5,15].

OCP is highly conserved among PBS-containing cyanobacteria [16,17]. At least three paralogous families of OCP exist: OCP1, OCP2, and OCPX [16]. The photoactivity and role of OCP have been mostly studied using OCP1s, especially that of *Synechocystis* PCC 6803. Recently, an OCP from another family, OCP2 from *Tolypothrix* PCC 7601 (also known as *Fremyella diplosiphon*), was characterized [16,18].

To recover the full capacity of the antenna, another protein is essential: the Fluorescence Recovery Protein (FRP) [19]. This protein helps in the detachment of the OCP1 from the PBSs and accelerates the conversion of OCP^R to OCP^O [19–21]. By contrast, OCP2 does not interact with FRP. The recovery reaction from OCP^R to OCP^O is fast in OCP2, even in the absence of FRP [16,18]. In addition, OCP2 does not need FRP to detach from the PBS [16,18].

OCP1 is ubiquitous and present in the cells even under low light conditions [22], but its concentration varies under different growth conditions. For example, the concentration of OCP1 depends on the intensity of growth light ([23] and references inside). General transcriptomic studies have shown that *ocp* transcription increases under different stress conditions ([23] and references inside). Almost all these studies were performed using the model organisms *Synechocystis* PCC 6803 (Synechococcales) and *Anabaena* PCC 7120 (Nostocales). The photoprotective mechanism in the filamentous strains that belong to Oscillatoriales, widely distributed in natural environments, is still unclear. In this study, we decided to characterize OCP and its related photoprotective mechanism in non-stressed and light-stressed cells of three different *Planktothrix* strains.

Planktothrix species are of particular environmental interest because they are able to form impressive blooms that strongly impact the uses of water for drinking water or recreational activities (see review [24]). One of the challenges related to the global expansion of cyanobacterial blooms is to understand the species adaptation to environmental changes. The adaptation mechanisms of cyanobacterial species to stressful environments related to human activities that cause warming, CO_2 increase, water pollution, and acidification, which decrease the phytoplankton biodiversity in aquatic ecosystems, have not yet been elucidated. All these changes have been demonstrated to have a large influence on cyanobacterial bloom formations. In addition to changes in lake functioning and biodiversity, these blooms can have adverse effects on human and animal health because of cyanotoxin-producing cyanobacteria (e.g., microcystins [MCs]). MCs are cyclic heptapeptides synthesized non-ribosomally by large multifunctional enzyme complexes containing both non-ribosomal peptide synthetase and polyketide synthase domains encoded by the *mcy* gene cluster [25]. Among bloom-forming cyanobacteria, filamentous *Planktothrix* species are distributed to the greatest extent in freshwater bodies worldwide, and they are common bloom-forming species [24]. Two main ecology-genotypes have been described within *Planktothrix*: a red pigmented ecotype (formerly named *Planktothrix rubescens*) that proliferates in deep lakes under low light intensity and temperature conditions [26] and a green pigmented ecotype (formerly named *Planktothrix agardhii*) that colonizes shallow lakes with higher intensities of light and temperature [26, 27]. To date, all red *Planktothrix* strains studied contain the *mcy* operon, indicating they are MC producers and suggesting that MCs could have an essential role in the survival of these strains [28]. Some green *Planktothrix* strains are MC producers, and others are not [29]. Previous results on green *Planktothrix* strains have shown that the non-MC genotypes are dominant under favorable growth conditions, whereas the MC genotypes grow better under stress conditions [30]. Therefore, MCs could have a protective role against oxidative and light stresses [28, 31].

Three *Planktothrix* strains were selected: two green strains PCC 10110 (MC producer) [32] and PCC 7805 (non-MC producer) [33], and one red strain, PCC 7821 (MC producer) [33]. We checked whether there is a correlation between the ecological niches in which these strains proliferate (shallow lakes with high light-temperate temperature for the green *Planktothrix* versus deep lakes with low light-low temperature for the red *Planktothrix*) and amplitude and kinetics of the OCP-related mechanism. We also studied the relationship among resistance to light stress, amplitude of the photoprotective mechanism, and/or presence of MCs. We used a multidisciplinary approach of biophysical (fluorescence measurements), molecular biology (mRNA quantification), and structural (transmission electron microscopy [TEM] and immunolocalization) studies to evaluate the changes that occur in Photosystem II (PSII) activity, OCP expression and concentration, related photoprotective mechanism, and MC concentration during light stress.

2. Material and methods

2.1. Strains and culture conditions

For the characterization of OCP and related photoprotection mechanism in *Planktothrix* strains, independent experiments were performed under controlled light conditions. The cells were grown in BG11 medium [34], maintained in a rotary shaker (40 rpm) at 22 °C, and illuminated by fluorescence white lamps (20 µmol photons $m^{-2} s^{-1}$).

For the big high light experiment, pre-culture of 1 L of each strain was grown in 2 L bottles for four weeks at 20 °C in a thermostatic room with a photon flux density of 6 µmol·m^{-2}·s^{-1} and a 13:11 h light:dark cycle; agitation was provided by magnetic stirring bars. After four weeks, the cultures reached an OD_{750nm} of about 0.2–0.3, and the high light experiment was conducted. T0 was sampled after 1 h of illumination at 6 µmol photons $m^{-2} s^{-1}$. Then, the cells were illuminated with strong white light (150 µmol photons $m^{-2} s^{-1}$) for 4 h (T4, 240 min). After this stress, the cells were transferred to control light conditions (6 µmol photons $m^{-2} s^{-1}$) for 6 h (T10, 600 min). Then the cells were transferred to dark during 11 h and illuminated again for 1 h with 6 µmol photons $m^{-2} s^{-1}$ (T24 of Fig. 8). Some cultures were maintained at 6 µmol photons $m^{-2} s^{-1}$ (control conditions, control). The experiment was performed in three different weeks, in triplicates, leading to nine biological replicates at each studied time.

In Fig. 3C and D, results of an independent high light stress experiment are shown. In this experiment, *Planktothrix* cells grown at 20 µmol photons $m^{-2} s^{-1}$ were illuminated by 4 h (240 min) with 250 µmol photons $m^{-2} s^{-1}$ of white light at a concentration of 0.4 OD_{800} in a PSI multi-cultivator (Photon System Instrument, Czech Republic). Three biological independent experiments were realized.

2.2. Chlorophyll a quantification and cell number and biovolume measurements

The cell abundance was estimated in triplicate by using the Mallassez-based method [35]. For chlorophyll *a* analysis, 5 mL of each culture was used and analyzed as described previously [36]. The cell volume of the *Planktothrix* strains was measured on the basis of their sizes [37].

2.3. Sample fixation and immunogold labelling

For TEM analysis, the cells were harvested by centrifugation and fixed with a mixture of 2% glutaraldehyde, 2% formaldehyde, 0.18 M sucrose, 0.1% picric acid in 0.1 M, pH 7.4, and Sorensen phosphate buffer (SPB) for 1 h. The cells were then washed three times with SPB.

Subsequently, they were washed with distilled water before dehydration in a graded ethanol series (30%, 50%, 70%, 90%, and 100%), with agitation and centrifugation. The samples were embedded in a non-antigenic Unicryl resin and sectioned (60 nm) using an ultra-microtome (Reichert-Jung Ultracut, Germany) with a diamond knife and transferred onto 150-mesh gold grids (for immunogold). For OCP localization in the *Planktothrix* cells, a polyclonal primary antibody against *Synechocystis* OCP (Covance) was used. To localize MCs, the monoclonal anti-MC antibody AD4G2 (Enzo), which is directed against the Adda group of the peptide, was used [38]. The sections were incubated with the primary antibodies (we used a dilution 1:250 for both antibodies) and then with the secondary antibodies (we used a dilution 1:500 for both antibodies) coupled to nanogold particles (6 nm ø for OCP and 10 nm ø for MCs). The prepared sections were stained with a saturated solution of uranyl acetate/50% ethanol for 15 min and washed three times in 50% distilled water/50% ethanol and finally twice in distilled water. The gold grids were then dried and examined using a transmission electron microscope (Hitachi HT-7700, Japan), and images were obtained using a digital camera (Hamamatsu, Japan).

2.4. Quantification and statistical analysis of immunogold labelling

To quantify the number of OCP and MC gold particles, the images were optimized before counting by using the Paint Shop Pro 8 software to eliminate elements that could interfere with the counting of the gold nanobeads. The counting was performed using the Icy Freeware Spot Detector plug-in parameterized with the appropriate settings to obtain exact detection (scale, detection threshold, and size filter). To obtain a number of detections per unit area (μm^2), the surfaces analyzed with Icy were calculated using the freeware Image J (NIH).

The statistical analysis was performed using the R Studio software. Because the data distribution was not normal (did not follow a Gaussian distribution), the following non-parametric tests were performed: the Wilcoxon test and Kruskal–Wallis test.

2.5. PAM fluorometer measurements

For characterization of the OCP-related photoprotection mechanism in *Planktothrix*, changes in the fluorescence levels were measured using 101/102/103-PAM (Walz, Effeltrich, Germany) with 650 nm detecting light. The cells were at a concentration of 2.5 µg chlorophyll *a* in a $1 \times 1\ cm^2$ stirred cuvette, and the experiments were performed at 20 °C. The dark-adapted cells (5 min) were illuminated with 85 µmol photons $m^{-2} s^{-1}$ of blue-green light (halogen white light filtered with a Corion cut-off 550-nm filter; 400 to 500 nm). Then, they were illuminated with strong blue light (blue-green, 1200 µmol photons $m^{-2} s^{-1}$). For fluorescence recovery, the cells were illuminated again with low intensities of blue-green light. Saturating flashes (400 ms × 5000 µmol photons $m^{-2} s^{-1}$ of white light) were provided to probe the maximum fluorescence level.

For the high light experiment, changes in the fluorescence levels were measured using a multicolor PAM (Walz, Effeltrich, Germany) with 590 nm detecting light. The cells were measured at a OD_{750nm} of about 0.2–0.3. The dark-adapted cells (5 min) were illuminated with diode blue light (440 nm, 53 µmol photons $m^{-2} s^{-1}$). Then, they were illuminated with strong blue light (440 nm, 2160 µmol photons $m^{-2} s^{-1}$).

Saturating flashes (400 ms × 12,000 µmol photons $m^{-2} s^{-1}$) were provided to probe the maximum fluorescence level. The fluorescence parameters used in the analysis were as follows: F_0, basal fluorescence; Fm′, maximum fluorescence in blue light; F_v = variable fluorescence = $F_m - F_0$.

2.6. Gel electrophoresis and western blotting

Total proteins and membrane-bound PBS proteins were analyzed with SDS-PAGE on 15% polyacrylamide/2 M urea gel in a Tris/MES system [39]. In each slot, a sample containing 3 µg of chlorophyll *a* was loaded. The OCP band was detected using an antibody against *Synechocystis* OCP (Covance).

2.7. RNA extraction and quantification by using quantitative real-time PCR

The culture (50 mL) was filtered through a polycarbonate membrane (diameter, 47 mm; pore size, 3 µm; Whatman Nucleopore), and the filter was transferred into 1.5 mL of RNAlater (Sigma) and stored at 4 °C overnight and then at −80 °C. For RNA extraction, the filter was cut into small pieces, and 850 µL of lysis buffer (ML lysis buffer, Macherey Nagel) was added. Extraction was performed using high-intensity ultrasonication (Ultrasonic Processor VCX 130; SONICS) twice for 30 s at 20% of the maximal power. The sample was vortexed after each 30 s pulse. After 5 min of incubation at room temperature, 700 µL of the sample was transferred into a NucleoSpin Filter with a silica membrane (Macherey Nagel) and centrifuged for 1 min; then, 600 µL of the supernatant was transferred, and 225 µL of ethanol was added. The total RNA was extracted using the NucleoSpin miRNA kit (Macherey Nagel), according to manufacturer's instructions. A large RNA fraction (> 200 nucleotides) was obtained and stored at −80 °C. Reverse transcription into cDNA and qPCR analyses were performed by the "Plateforme de PCR Quantitative à Haut Débit Genomic Paris Centre, Ecole Normale Supérieure." The primers used for *frp* and *ocp* expression studies are listed in Table S1. Relative quantification of each gene expression level was normalized according to *rpoC*, *gyrB*, and *rpsL* expression. The relative mRNA expression was evaluated using the $2_T^{-\Delta\Delta C}$ method [40].

2.8. Intracellular MC concentration

Ten milliliters of the MC-producing *Planktothrix* strains was centrifuged (4000 rpm, 10 min), and the pellet was freeze-dried. The lyophilized cells were weighed and then sonicated for 2 min in 80% methanol with a constant ratio of 100 µL of solvent to 1 mg of dried biomass and centrifuged at 4 °C (12,000 × *g*; 5 min). Two microliters of the supernatant representing the metabolite extracts was then analyzed in triplicate by using ultra high-performance liquid chromatography (UHPLC Ultimate 3000; ThermoFisher Scientific) and a Polar Advances II 2.5 pore C_{18} column (Thermo) at 300 µL·min^{-1} flow rate and a linear gradient of acetonitrile in 0.1% formic acid (5 to 90% in 21 min) coupled with a high-resolution mass spectrometer. The eluted metabolite contents were analyzed using an electrospray ionization hybrid quadrupole time-of-flight (ESI-QqTOF) high-resolution mass spectrometer (Maxis II ETD, Bruker) on positive autoMS/MS mode with information-dependent acquisition (IDA) between 2 and 16 Hz speed, according to the relative intensity of the parent ions, in consecutive cycle times of 2.5 s and active exclusion of previously analyzed parents. The data were analyzed with the DataAnalysis 4.4 software for internal recalibration (< 0.5 ppm), and MGF export was generated from the MS/MS spectra between 1 and 15 min. Microcystin annotation was attempted according to the precise mass of the molecules and their respective MS/MS fragmentation patterns. The most intense MC variants were semi-quantified according to similar LC-MS/MS analyses performed on positive broad-band CID fragmentation mode (bbCID) at 2 Hz, and the raw data were searched with the TASQ 1.3 software (Bruker, Germany) for targeted screening and quantification according to a list of targeted most-intense analytes (based on the accuracy of their mass, isotopic pattern, retention time, and detection of qualifying fragment ions). The effects of high light on MC concentrations were tested using multifactorial analysis of variance (two-way ANOVA), and multiple comparisons were conducted with Tukey-HSD tests. Normality and homogeneity of variance were checked prior to the data analysis.

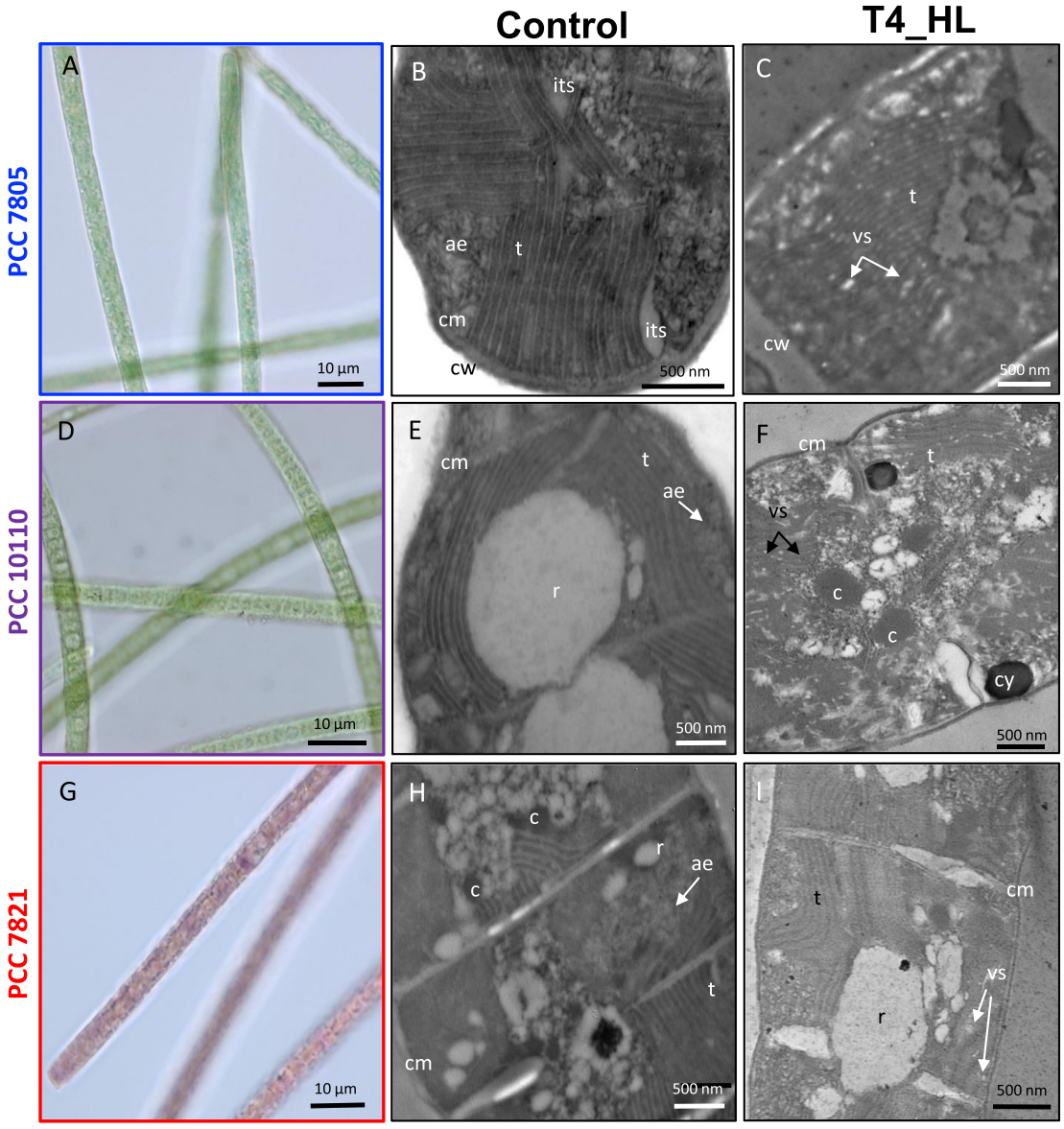

Fig. 1. *Planktothrix* strains characteristics in control and high-light stress. Light microscopy (A, D, G) and TEM (B, C, E, F, H, I) of *Planktothrix* strains PCC 7805 (green phenotype), PCC 10110 (green phenotype) and PCC 7821 (red phenotype) in control conditions (Control) and after 4 h of high-light (T4_HL) stress. A: light microscopy of *Planktothrix* PCC 7805. B, C: TEM sections of *Planktothrix* PCC 7805. D: light microscopy of *Planktothrix* PCC 10110. E, F: TEM sections of *Planktothrix* PCC 10110. G: light microscopy of *Planktothrix* PCC 7821. H, I: TEM sections of *Planktothrix* PCC 7821. t: thylakoids, r: reserves (lipids, polyphosphates, poly-β-hydroxybutyrate), ae: aerotopes, cm: cytoplasmic membrane, c: carboxysome, cy: cyanophycin granule, vs: clear vesicle.

3. Results and discussion

3.1. Planktothrix strain characteristics under control and high light conditions

The aspects and ultrastructural organizations of the three studied *Planktothrix* strains are presented in Fig. 1 and Table 1. *Planktothrix* PCC 7805 and PCC 10110 appear green (Fig. 1A, D) under a light microscope with phycocyanin (PC) as the major phycobiliprotein, whereas *Planktothrix* PCC 7821 is red (Fig. 1G) with phycoerythrin (PE) as the major phycobiliprotein. The main MC variants of *Planktothrix* PCC 10110 are [Asp3, Dha7] MC-YR (34.3%), [Dha7] MC-YR (30.8%), and MC-YR (34.8%), and those of *Planktothrix* PCC 7821 are (Asp3) MC-RR (45.8%) and (D-Asp3) MC-LR (54.2%) (Table 1). The diversity of MC variants between the strains could be a consequence of genetic variations within the different domains of the *mcy* gene cluster. These genetic variations are the result of modifications and combinations within the MC synthesis pathway [31, 41]. The MC variants have been speculated to be different in red or green *Planktothrix*; however, environmental or culture conditions and physiological status may also influence the proportion of MC variants ([41] and Kim Tiam et al., pers. comm.).

The TEM images (Fig. 1; supplementary Figs. S4–S6) of the three *Planktothrix* strains clearly show the ultrastructure of the thylakoids, which consist of two electron-dense layers and an electron-transparent one between them. Other main components were observed within the cells: aerotopes or gas vesicles (which promote floatation of the filament within the water column), carboxysomes (polyhedral or dense bodies), cyanophycin granules (reserves of nitrogen), reserves (e.g., glycogen, lipid, or poly-β-hydroxybutyrate acting as a source of carbon and energy), and polyphosphate granules (reserves of phosphorus) [42, 43]. Other inclusions surrounded by cytoskeleton filaments (e.g., microtubules and microfilaments) were also observed. Under the control conditions, the thylakoid arrangement differs in the three *Planktothrix*

Table 1
Planktothrix strains main characteristics under control and after 4 h (240 min) of high-light stress conditions.

Planktothrix	PCC 7805		PCC 10110		PCC 7821	
Phenotype (color)	Green		Green		Red	
Major phycobiliprotein	Phycocyanin		Phycocyanin		Phycoerythrin	
MC variants	–		[Asp3, Dha7] MC-YR (34.3%) [Dha7] MC-YR (30.8%) MC-YR (34.8%)		(Asp3) MC-RR (45.8%) (D-Asp3) MC-LR (54.2%)	
Cell biovolume (μm^3)	72.4		77.6		56.8	
Chl *a* $pg \cdot cell^{-1}$	0.21		0.32		0.35	
DW $pg \cdot cell^{-1}$	0.22		0.40		0.34	
	Control	High-light	Control	High-light	Control	High-light
Ultrastructural characteristics						
Thylakoids	Parallels, well defined, in the whole cells, inter-thylakoidal spaces	Swelled, small vesicles	Parallels, well defined, large reserves area	Swelled, less compact	Parallels, not well defined,	Swelled, less compact with vesicles between thylakoids
Reserves granules	Few, small		Abundant, large		Abundant, small	
OCP (number μm^2 thylakoid)	19.3 ± 3.4	103.2 ± 50.2	80.7 ± 33.5	39.2 ± 16	17.4 ± 8.1	39.5 ± 10.4
MC (number μm^2 thylakoid)	–	–	4.2 ± 1.4	1.5 ± 1.2	2.7 ± 1.0	1.9 ± 0.7
OCP/MC	–	–	19.2	26.1	6.4	20.8

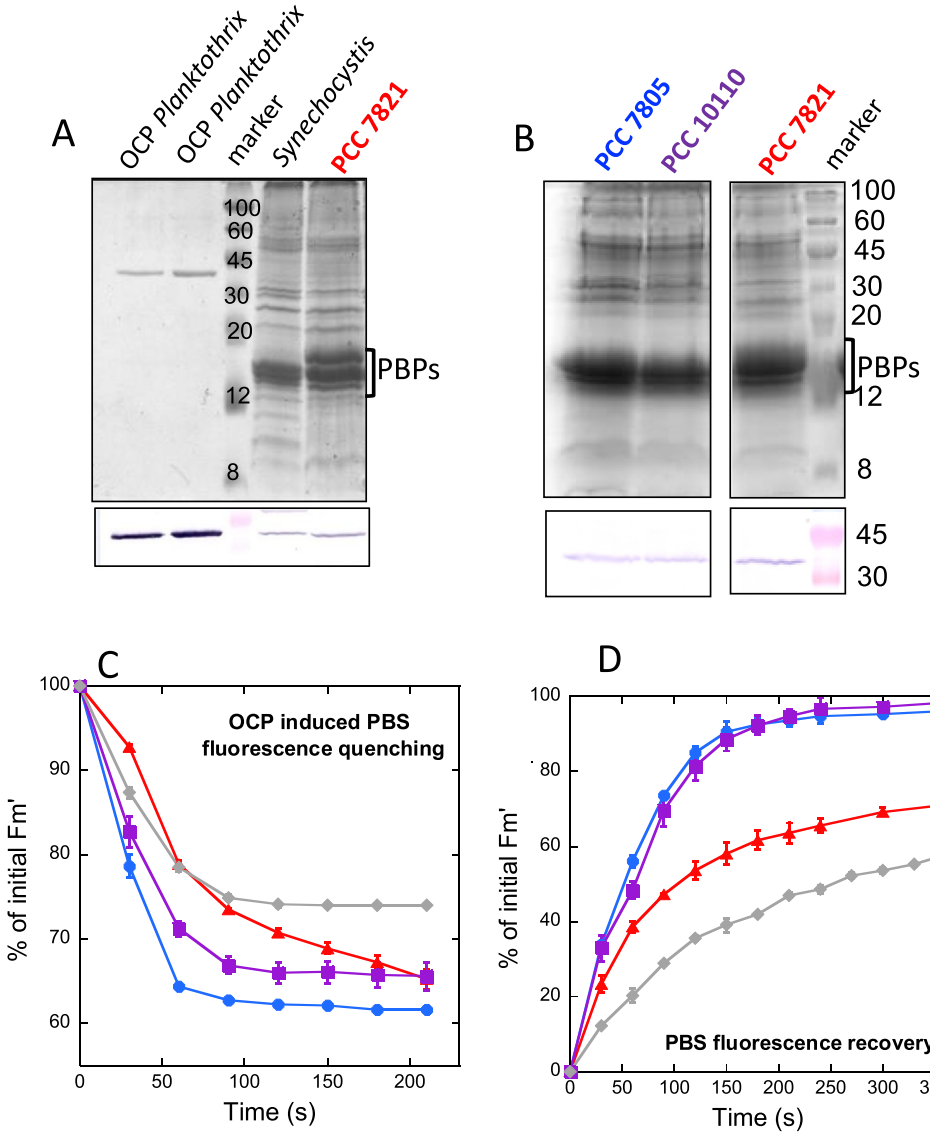

Fig. 2. The OCP and the related photoprotective mechanism. (A and B) Gel electrophoresis and OCP detection by anti-*Synechocystis* OCP. (A) isolated *Planktothrix* PCC 7805 OCP (slots 1 and 2, 0.5 and 1 µmol respectively); (slots 3–4) isolated membrane-bound phycobilisome complexes of *Synechocystis* PCC 6803 (3) and *Planktothrix* PCC 7821 (4). (B) total cell protein of *Planktothrix* PCC 7805, *Planktothrix* PCC 10110 and *Planktothrix* PCC 7821. The cells for these experiments were grown at 20 µmol photons $m^{-2} s^{-1}$ (C and D) PBS fluorescence quenching induced by strong blue light (1200 µmol photons $m^{-2} s^{-1}$) in *Planktothrix* cells grown at 20 µmol photons $m^{-2} s^{-1}$ (C) and fluorescence recovery under low blue light was measured by a 101/102/103-PAM (Walz, Effeltrich, Germany) with 650 nm detecting light (D). *Planktothrix* PCC 7805 (blue circles), PCC 10110 (violet squares), PCC 7821 (red triangles) and *Synechocystis* PCC 6803 (gray diamond).

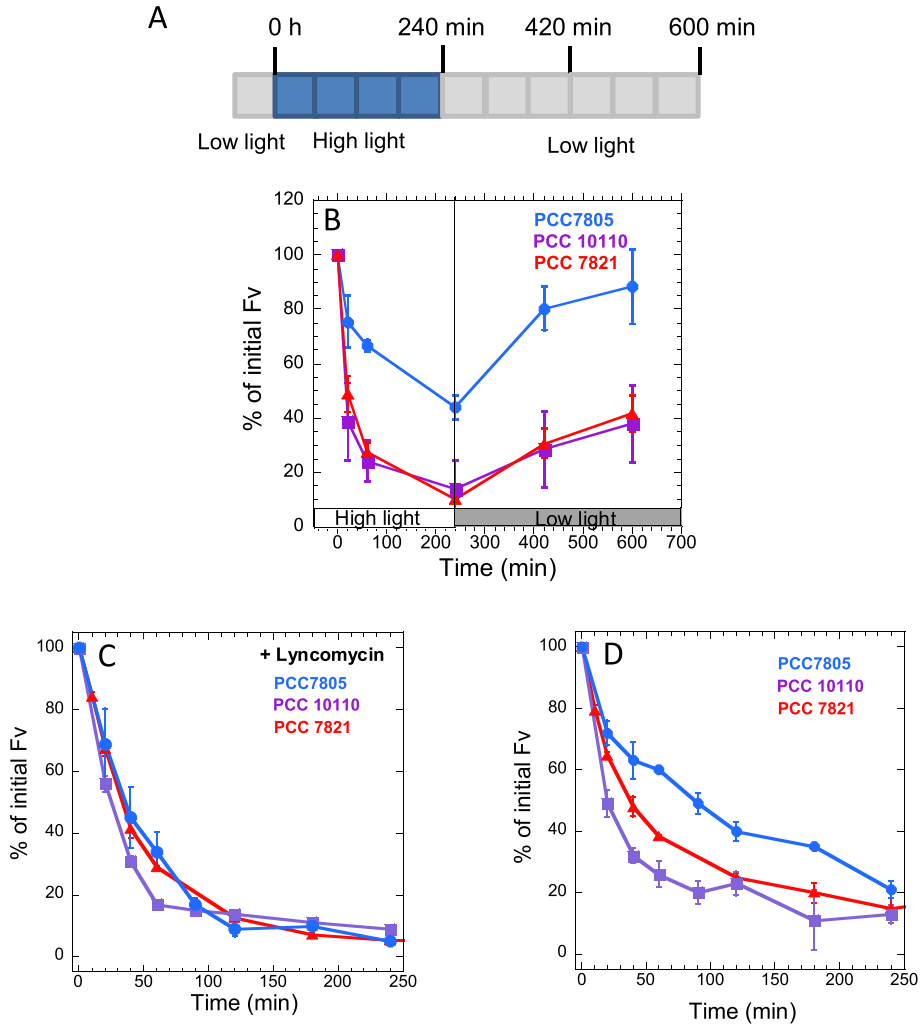

Fig. 3. PSII activity decrease during high-light stress. (A) Scheme of the high-light stress and recovery experiment. Cells grown at 6 µmol photons $m^{-2} s^{-1}$ were exposed to 150 µmol photons $m^{-2} s^{-1}$ (B) The decrease and increase of PSII activity during the experiment was followed by measuring dark Fv measured using a multicolor-PAM. The graph shows the mean of three independent biological experiments with technical triplicates (C and D) Independent experiments in which the cells grown at 20 µmol photons $m^{-2} s^{-1}$ (at OD_{800} = 0.4) were light stressed (250 µmol photons $m^{-2} s^{-1}$ white light) in the presence (C) or absence (D) of lyncomycin (0.4 mg/mL) that inhibits PSII repair. *Planktothrix* PCC 7805 (blue circles), PCC 10110 (violet squares), PCC 7821 (red triangles). The graph shows the mean of three biological independent experiments. The error bars represent SD.

strains. In *Planktothrix* PCC 7805, the thylakoids are well-defined, in groups of > 6 units, and distributed in the whole cell (Fig. 1B, supp. Fig. S4). Several interthylakoidal spaces are observed in this strain. In *Planktothrix* PCC 10110, the thylakoids are also arranged in parallel lines; however, they are less compact, with numerous interthylakoidal spaces and a remarkably large "white" area, suspected to be poly-β-hydroxybutyrate reserves (Fig. 1E, supp. Fig. S5). Finally, in the red *Planktothrix* PCC 7821, the thylakoids seem to be shorter and distributed all over the cell with smaller fragmented vesicles and reserve granules (Fig. 1H, supp. Fig. S6).

Cell exposure to high light induced important ultrastructural modifications (Fig. 1C, F, I; supp. Figs. S4–S6). In all the strains, the thylakoids were swollen (less compact) after 4 h of light stress. In addition, *Planktothrix* PCC 7805 and PCC 7821 showed a large increase in clear electron vesicles between the thylakoids (Fig. 1C and I; supp. Figs. S4 and S6). According to [42], these small vesicles could contain poly-β-hydroxybutyrate. In *Planktothrix* PCC 10110, the large reserve area (Fig. 1F, gray areas in the image) appears to be smaller after light stress. These ultrastructural responses of *Planktothrix* to high light stress have already been described in other cyanobacteria (e.g., *Anabaena variabilis* CALU 458) [43]; the authors showed that the thylakoids swelled, lost their parallel orientation, and formed vesicles under high light intensity. The authors suggested there could be a correlation among the organization of the thylakoid system, chlorophyll content, and photosynthesis rate as well as between the ultrastructure and chemical composition of the thylakoids under various illumination conditions [43].

3.2. OCP and related photoprotective mechanism in the Planktothrix strains

The genomes of the three strains and of all the *Planktothrix* strains sequenced to date have only one *ocp* gene and one *frp* gene [16]. The *Planktothrix* OCP belongs to the OCP1 clade [16]. The OCP proteins are highly conserved among the three studied *Planktothrix* strains (97.5–98.7% similarity); only a variation of nine amino acids was observed between the three protein sequences (Supplementary Fig. S1).

Preliminary independent experiments were performed to confirm the presence of the OCP and the OCP-related NPQ mechanism in the three studied *Planktothrix* strains. The cells for these experiments were grown in 250 mL Erlenmeyer's maintained in a rotary shaker (40 rpm) at 22 °C, and illuminated by fluorescence white lamps (20 µmol photons $m^{-2} s^{-1}$).

The presence of OCP in the three strains was detected using gel electrophoresis and western blot analysis with the OCP antibody against *Synechocystis* OCP. This antibody identified the isolated *Planktothrix* OCP (Fig. 2). In Fig. 2A, the presence of OCP in membrane-bound phycobilisome (MP) complexes isolated from *Synechocystis* and *Planktothrix* PCC 7821 is shown. In Fig. 2B, the presence of OCP is detected in total cell protein of the three *Planktothrix* strains. In each slot of the gel, the same quantity of chlorophyll *a* (3 µg), was loaded. Although the method was not quantitative because the specificity of the antibody could differ between strains, we always observed a stronger OCP band from the total cell protein extracted from *Planktothrix* PCC 7821.

The OCP-related photoprotective mechanism, induced by strong

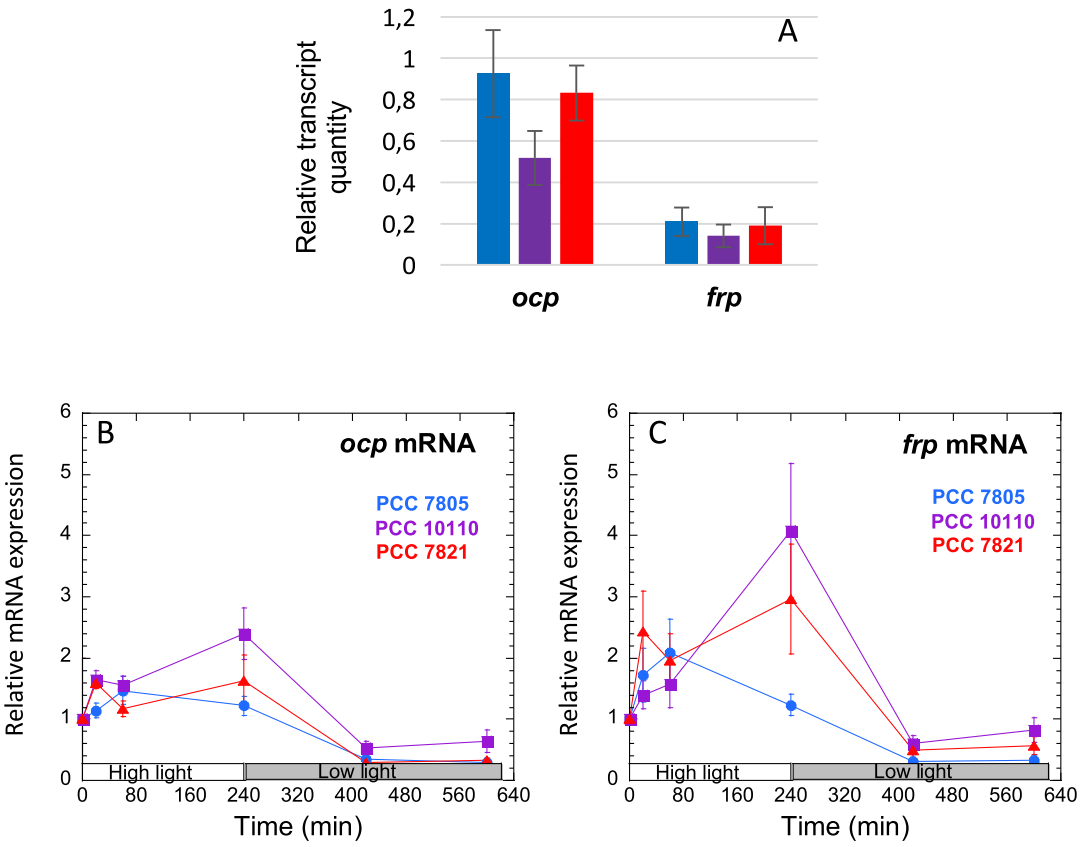

Fig. 4. Relative expression of *ocp* and *frp* genes under high light treatment and recovery. (A) Relative mRNA expression level at T0 normalized against three reference genes (*rpo*C, *gyr*B and *rps*L) for *Planktothrix* PCC 7805 (blue), PCC 10110 (violet), PCC 7821 (red). (B and C) Relative expression compared T0 of *ocp* (B) and *frp* (C) normalized against three reference genes (*rpo*C, *gyr*B and *rps*L), generated using the $2^{-\Delta\Delta C_T}$ method, during the high-light stress experiment for the three *Planktothrix* strains. *Planktothrix* PCC 7805 (blue circles), PCC 10110 (violet squares), PCC 7821 (red triangles). The graph present the mean of three biological independent experiments.

blue-green or white light, increases the thermal dissipation of excess energy absorbed by the PBS. This process is accompanied by a decrease in PBS fluorescence that was measured by a 101/102/103 PAM (Walz, Effeltrich, Germany) with 650 nm detecting light. The dark-adapted *Planktothrix* cells were first illuminated with low intensities of blue-green light that induced an increase in fluorescence due to transition to State I; then, they were illuminated with strong blue-green light to induce the OCP-related mechanism (example of PAM traces in supp. Fig. S2). A decrease in the maximal fluorescence (Fm′) under strong light in the three *Planktothrix* strains was observed (Fig. 2C). When the cells were then illuminated again with low intensities of blue-green light, an increase in maximal fluorescence was detected related to the recovery of full antenna capacity (Fig. 2D). The rate and amplitude of fluorescence quenching under strong light as well as the rate of fluorescence recovery under dim light observed in the green PCC 7805 and PCC 10110 strains were similar (Fig. 2C and D). In contrast, the rate of fluorescence quenching was slower in the red PCC 7821 strain, although the final amplitude of the quenching was equal to those observed in the green strains (Fig. 2C). This could be due, at least partially, to the presence of PE in the PBS of PCC 7821. PE absorbs green light and reduces the light available for photoactivation of OCP. However when the OCP-related NPQ mechanism was compared in different marine *Synechococcus* strains containing only PC or PC and different types of PE, it was shown that the presence of PE is not always related to lower OCP-related photoprotection [44]. One PE containing strain, presented larger fluorescence quenching than the blue-green strain, other one the same and the third one less fluorescence quenching. Thus, most probably, the difference in the OCP-related NPQ between green and red *Planktothrix* strains is related to their ecological niches. The green strains, which live in shallow lakes and can be exposed to the highest light intensities, are able to induce a fast quenching of excess absorbed energy; the quenching is much faster than that by the red strain which in nature grows in deep lakes under low light conditions. The rate of fluorescence recovery was also slower in the red strain (Fig. 2D).

The blue-green light induced PBS fluorescence quenching, and the fluorescence recovery was compared to those of *Synechocystis* PCC 6803 cells, which is the most studied cyanobacterial strain (Fig. 2C and D). The amplitude of the fluorescence quenching was larger in the *Planktothrix* strains than in *Synechocystis*, and the fluorescence recovery was faster. The rate and amplitude of fluorescence quenching depend on the concentration of photoactivated OCP^R, which depends on the total concentration of OCP, light intensity, and ratio of OCP to FRP. The affinity of OCP for the PBS of *Synechocystis* PCC 6803 also plays an important role in the rate and amplitude of OCP-induced quenching. All these factors could be different in the red and green *Planktothrix* and *Synechocystis*, leading to different quenching amplitudes and recovery rates even when they seem to have similar OCP to chlorophyll *a* ratios. Also *Arthrospira maxima* and *Synechocystis* PCC 6803 strains presented different amplitudes of the OCP related photoprotection although the OCP concentrations were similar [45].

3.3. PSII activity and ocp and frp mRNA levels during high-light stress and recovery

Once characterized the OCP-related NPQ mechanism in the *Planktothrix* strains, we studied the high light sensitivity of these strains and followed the behavior of this mechanism during a light stress and

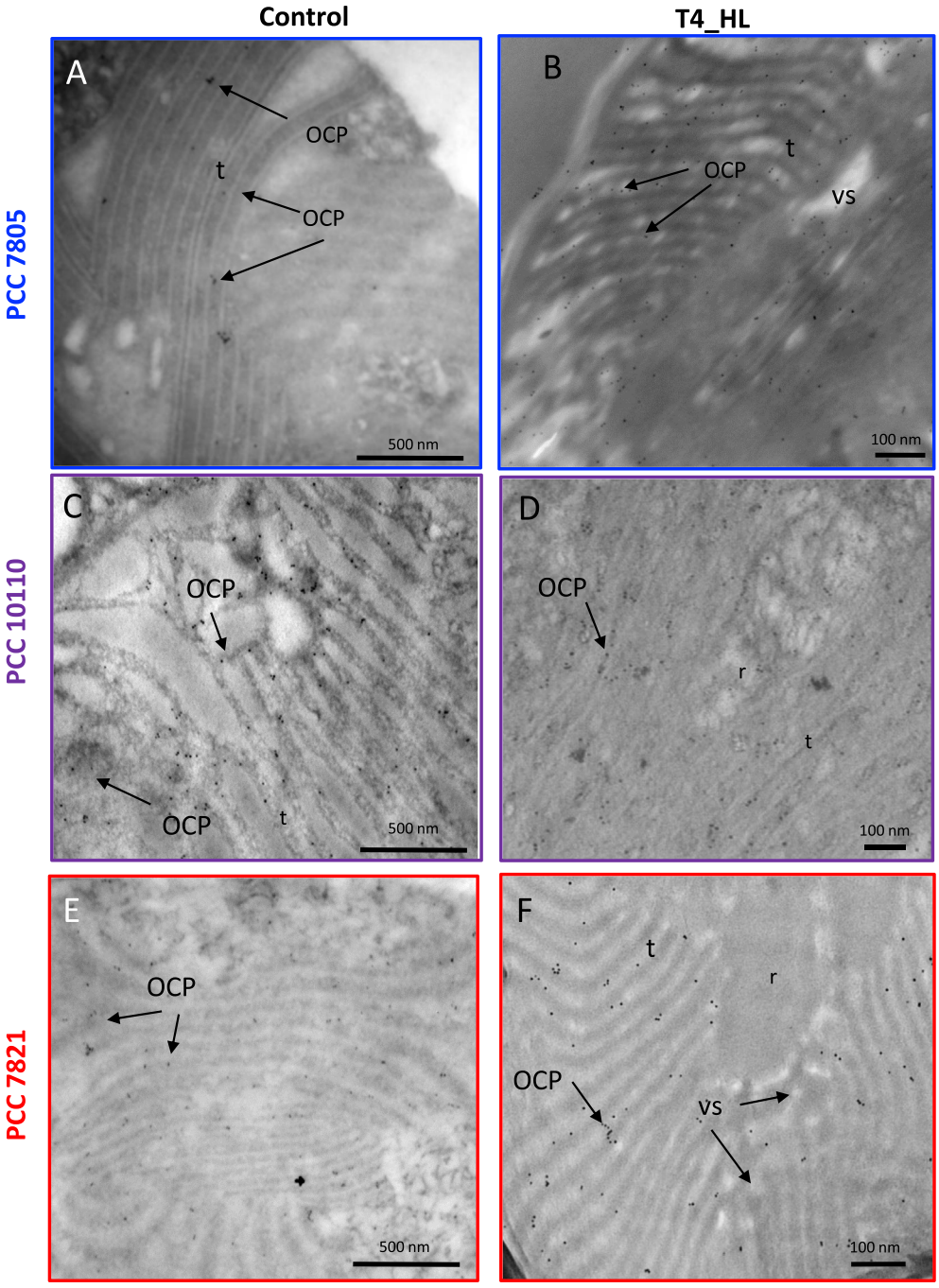

Fig. 5. Immunogold labelling of OCP (6 nm gold particles) in control and high-light stress. TEM micrographs of *Planktothrix* PCC 7805 (A, B), PCC 10110 (C, D) and PCC 7821 (E, F) in control conditions (Control) and after 4 h of high-light (T4_HL) stress with a clear and specific OCP localization on the thylakoids membranes. t: thylakoids, r: reserves (lipids, polyphosphates, poly-β-hydroxybutyrate …), vs: clear vesicle.

recovery. For this, the three strains were grown in a light:dark (13:11 h) regimen. The T0 was sampled after 1 h of illumination at 6 µmol photons $m^{-2} s^{-1}$. Then, the cells were illuminated with strong white light (150 µmol photons $m^{-2} s^{-1}$) during 4 h (T4, 240 min). After this stress, the cells were transferred to low light conditions (6 µmol photons $m^{-2} s^{-1}$) during 6 h. Control cells were maintained under low light conditions during the period of light stress. PSII activity was evaluated by measuring the decrease in dark variable fluorescence (Fv) during the high light-stress experimentation with a multicolor PAM fluorometer with 590 nm detecting light (Fig. 3, examples of PAM traces in supplemental Fig. S3). *Planktothrix* PCC 7805 lost only 60% of the initial dark Fv after 4 h (240 min) of high-light stress; the other two lost 90%, indicating that this strain is more resistant to photoinhibition (Fig. 3B). During the 6 h of recovery under low intensities of white light, only *Planktothrix* PCC 7805 recovered almost all the lost dark Fv; the other two recovered only 30% (600 min in Fig. 3B).

To elucidate whether the higher resistance to high light in *Planktothrix* PCC 7805 was related to less PSII photodamage or better recovery, the three *Planktothrix* strains were photoinhibited in the absence or presence of lyncomycin in independent experiments. Lyncomycin is an inhibitor of protein synthesis, and it inhibits the replacement of damaged proteins, especially D1 protein. In these experiments, *Planktothrix* cells grown at 20 photons $m^{-2} s^{-1}$ were illuminated during 4 h (240 min) with 250 µmol photons $m^{-2} s^{-1}$ in at a

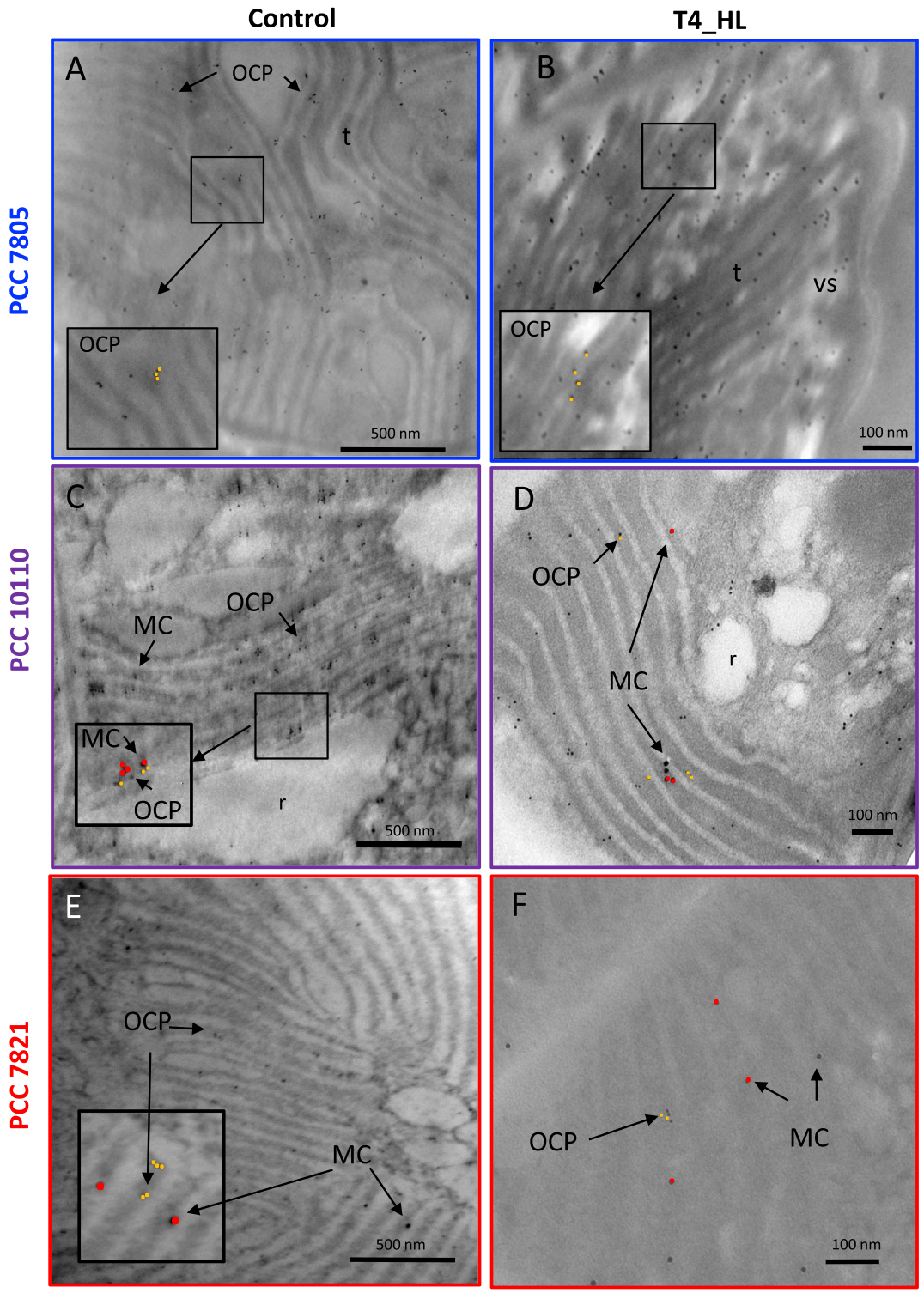

Fig. 6. Immunogold labelling of OCP (6 nm gold particles) and MC (10 nm gold particles) in control and high-light stress. TEM micrographs of *Planktothrix* PCC 7805 (A, B), PCC 10110 (C, D) and PCC 7821 (E, F) with co-immunolocalization of OCP (6 nm, orange dot) and MC (10 nm, red dot) in control conditions (Control) after 4 h of high-light (T4_HL) stress with a clear localization of OCP and MC on the thylakoids membranes for the two MC-producing strains PCC 10110 and 7821. t: thylakoids, r: reserves (lipids, polyphosphates, poly-β-hydroxybutyrate …), vs: clear vesicle.

concentration of 0.4 OD_{800} in a PSI multi-cultivator (Photon System Instrument, Czech Republic). In the presence of lyncomycin, the decrease in PSII activity was similar among the three strains (Fig. 3C). In the absence of lyncomycin, PSII activity decreased slower in *Planktothrix* PCC 7805 (Fig. 3D), indicating that this strain possesses a better recovery machinery.

The quantification of *ocp* and *frp* mRNAs by using quantitative real-time PCR showed that the concentration of *ocp* mRNAs is largely higher than that of *frp* mRNAs at T0 (Fig. 4). This is in accordance with other studies showing that OCP concentration is largely higher than that of FRP in *Synechocystis* cells [19, 20]. This is essential for the photoprotective mechanism: a high concentration of FRP completely inhibits

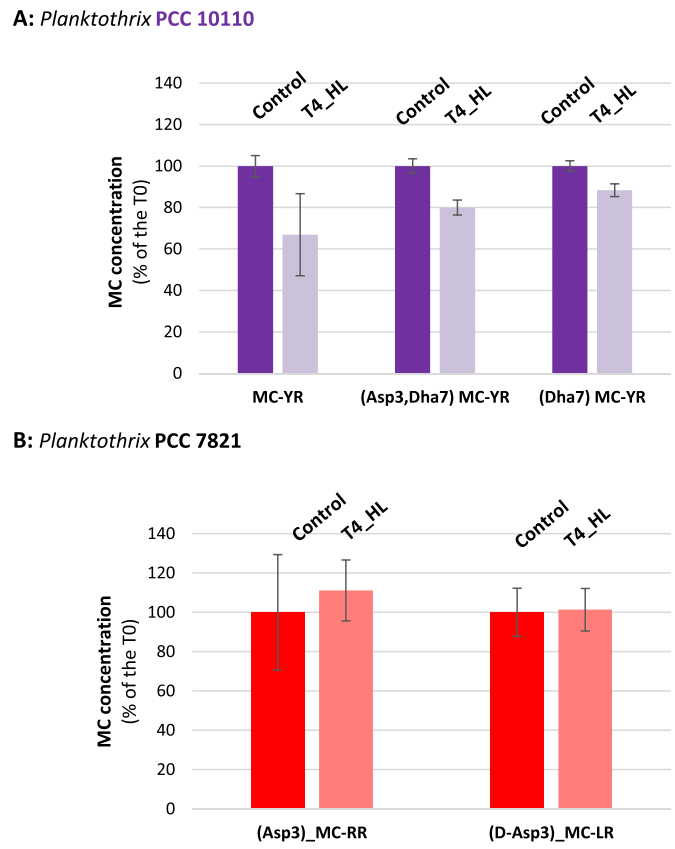

Fig. 7. Microcystin concentrations obtained by mass spectrometry (calculated in % of the T0) in control (strong colors) and 4 h (240 min) high-light (HL) stressed (dim colors) cells for the *Planktothrix* strains PCC 10110 (A, green) and PCC 7821 (B, red).

the photoprotective mechanism by rapidly reconverting the OCP^R to OCP^O before it can attach to the PBS [20].

Our study revealed that *ocp* mRNA concentration increased in the three strains during the 4 h (240 min) of high-light stress (Fig. 4B). The kinetics and amplitude of this increase were different in each strain. In PCC 10110 and PCC 7821, the maximum concentration of *ocp* mRNA was observed after 4 h (240 min). In PCC 7805, the maximum concentration was detected at 1 h (60 min). The increase was higher in *Planktothrix* PCC 10110 than in the other two strains (2.5-fold versus 1.5-fold). During the recovery process, the concentration of *ocp* mRNA decreased to lower than that at the beginning of the experiments. The *ocp* expression also increases under high light stress in *Synechocystis* and *Tolypothrix* cells [16, 46]; by contrast, there is limited information on the regulation of *frp* because of its low mRNA concentration. *ocp* and *frp* possess their own promoters and could be regulated independently [20]. Nevertheless, changes in the concentration of *frp* mRNA followed the same pattern as that of *ocp* mRNA although unexpectedly, the increase in *frp* mRNA was higher than that of *ocp* mRNA (Fig. 4C). In *Planktothrix* PCC 10110 and PCC 7821, the *frp* mRNA concentration largely increased during the 4 h of high-light stress, and it then decreased during the recovery time under control light conditions. In *Planktothrix* PCC 7805, the *frp* mRNA concentration was maximum after 1 h of high-light stress, and it then decreased.

In conclusion, our results demonstrated that, in *Planktothrix* cells, *ocp* and *frp* are co-regulated: both increase during light stress and then decrease during the recovery.

3.4. TEM and detection of OCP and MC by using immunogold

For OCP and MC localization in the *Planktothrix* cells, a polyclonal and monoclonal primary antibody were used, respectively. OCP was clearly localized in the thylakoid membrane region in the three *Planktothrix* strains (Fig. 5 and supp. Figs. S5–S7). This confirmed the cell localization of OCP, which has been previously observed in only *Synechocystis* [22] (see also supp. Fig. S4). In multiple places, two or several OCPs were grouped.

The MC were also mainly located in the thylakoid region of the two MC-producing *Planktothrix* PCC 10110 and 7821 (Fig. 6), as observed in two other cyanobacteria [47]. No MC labeling was observed in the non-MC-producing P*lanktothrix* PCC 7805 strain (Fig. 6). This negative immunostaining was considered as the negative control, and it validates the method of immunolocalization of MC. The number of MC detected is low (Fig. 6) and is in concordance with the low concentration of MC measured in mass spectrometry (data not shown).

To measure the changes in OCP and MC concentrations during high-light stress, the gold nanoparticles attached to OCP and MC antibodies were counted in the thylakoid region. Then, the numbers of OCP and MC particles were compared at T0 and T4 (240 min) in the three strains (Table 1). Analysis of OCP particle number per surface of the thylakoid showed a significant increase at T4 in *Planktothrix* PCC 7805 and PCC 7821 because of the light stress (5.3- and 2.3-fold, respectively; Table 1). Surprisingly, although *ocp* mRNA concentration also increased in *Planktothrix* PCC 10110, (Fig. 4), a significant decrease in OCP particles per surface of the thylakoid (2-fold) was observed in this strain (Table 1). We suspected that thylakoid disorganization in *Planktothrix* PCC 10110 induced by high-light stress (Fig. 1I; supp. Fig. S6) with less compacted thylakoid can have an effect on the OCP number per surface of the thylakoid.

By contrast, MC immunolabeling decreased during the high-light stress in *Planktothrix* PCC 10110, whereas it remained more or less stable in *Planktothrix* PCC 7821. This is consistent with the mass spectrometry measurements performed in parallel; the mean MC-variant concentrations decreased, for the three MC-variants, in PCC 10110 (Fig. 7).

3.5. OCP-related photoprotection during light stress and recovery

The OCP-related fluorescence quenching induced in T0, T1 (60 min, HL), and T4 (240 min, HL) in the three studied strains is shown in Fig. 8. In the T0 samples of the three strains, 35% of the fluorescence was decreased after 110 s of strong blue-green light illumination (Fig. 8A). As observed in the independent experiments (Fig. 3), the decrease in blue-green light-induced quenching was slower in the red *Planktothrix* PCC 7821 than in the green strains at T0. Interestingly, although the concentration of OCP per μm^2 of thylakoids (Table 1 and Figs. 5 and 6; supp. data Figs. S5–7) was largely higher in PCC 10110 (80 OCP μm^2 of thylakoids) than in PCC 7805 (17 OCP μm^2 of thylakoids), the amplitude of quenching was similar in the two strains. This could be at least partially explained by the higher concentration of PBS and photosystems in the PCC 10110 strain (supp. Fig. S8). Thus, the ratio of OCP to PBS could be similar in PCC 10110 and PCC 7805 strains.

At T4 (240 min) after high-light stress, strong blue-green light induced less fluorescence quenching than at T0, especially in *Planktothrix* PCC 7821 and PCC 7805 (Fig. 8B and C). This was completely unexpected in these two strains, in which the number of OCP particles increased during stress. A possible explanation is that OCP also binds to PBS connected to non-fluorescent inactive PSII. In the PBS, the fluorescence could be already quenched by the photosystems, and the OCP activity was invisible. On the other hand, these results can also suggest that, after prolonged light stress, the OCP-PBS interaction was affected leading to less photoprotection. Previously, this mechanism was proposed to be especially effective in protecting cyanobacteria under fluctuating light conditions [44]. After 20 h of recovery, the initial amplitude of fluorescence quenching was recovered (Fig. 8). The rates and amplitudes of fluorescence quenching in the cells maintained under

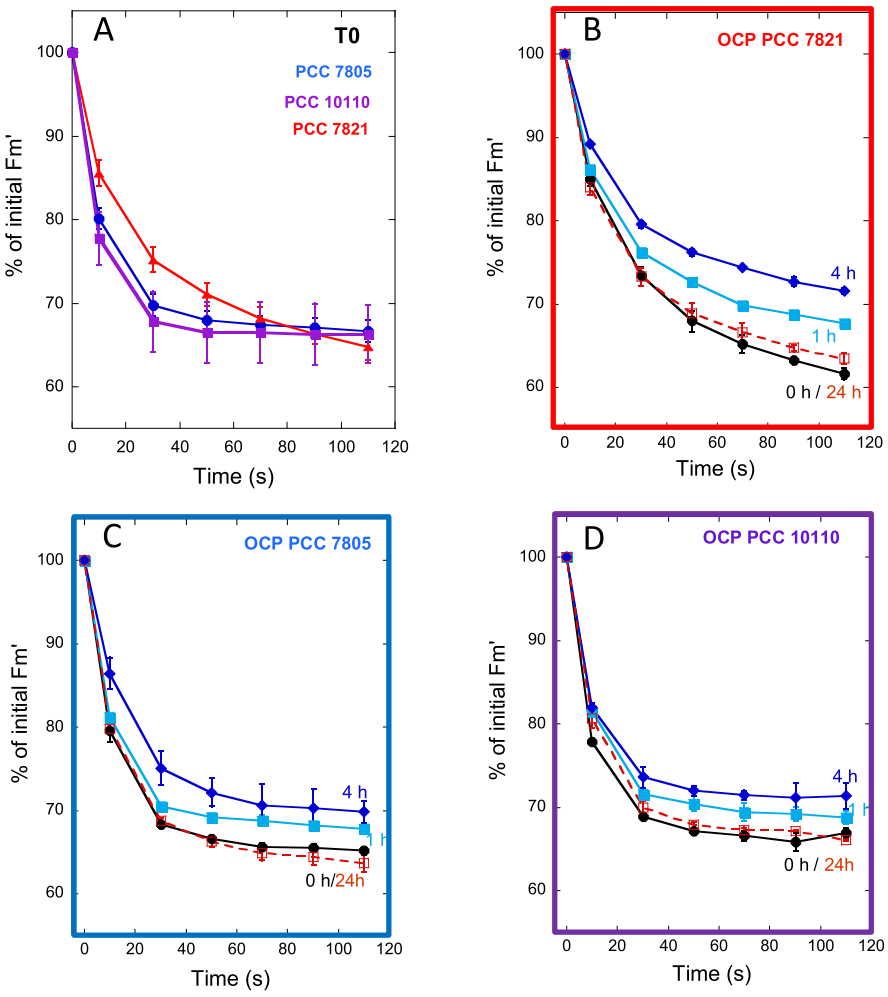

Fig. 8. OCP-related photoprotective mechanism during high-light stress and recovery. Cells grown at 6 µmol photons $m^{-2} s^{-1}$ were exposed to 150 µmol photons $m^{-2} s^{-1}$ white light for 4 h (light stress) and then to 6 µmol photons $m^{-2} s^{-1}$ for recovery. Fm′ decrease induced by cell exposition to strong blue light (440 nm; 2160 µmol photons $m^{-2} s^{-1}$) measured using a multicolor-PAM. (A) Comparison of the Fm′ decrease in the three studied strains at T0. *Planktothrix* PCC 7805 (blue circles), PCC 10110 (violet squares), PCC 7821 (red triangles). (B to D) strong blue light induced Fm′ decrease in samples collected at T0 (black circles), T1 (60 min light stress) (blue squares), T4 (240 min light stress) (violet diamonds) and T24 (20 h (1200 min) of recovery under low light) (open orange squares) of the experiment from *Planktothrix* PCC 7821 (B), PCC 7805 (C) and PCC 10110 (D).

low light intensities or transferred to a higher temperature were similar during the 10 h (600 min) of the experiment (supp. Fig. S9).

4. Conclusions

The OCP present in the thylakoid region of the three *Planktothrix* strains was able to induce a large PBS fluorescence quenching upon photoactivation by strong blue-green light. Induction of the photoprotective mechanism was faster in the two green *Planktothrix* strains than in the red one. In addition, recovery was faster in the green *Planktothrix* strains. These different phenotypes could be related to the specific ecological niches for green and red *Planktothrix* ecotypes. The first ones proliferate in eutrophic, shallow lakes under light-fluctuating conditions and need more flexibility in their photoprotective mechanisms than the red ones that grow in deep lakes with lower light intensities and fewer fluctuations.

We compared the two green strains and did not observe a direct correlation between the OCP-related photoprotective mechanism and resistance to prolonged exposure to high light. Although the rate of induction and amplitude of the PBS fluorescence quenching were similar in both species, *Planktothrix* PCC 7805 was more resistant to light stress than *Planktothrix* PCC 10110. This seems to be related to a better capacity for repairing the photodamaged PSII in PCC 7805.

A simple comparison of the concentration of OCP per chlorophyll (or per thylakoid surface) in different cyanobacteria strains does not provide an idea of the importance and characteristics of OCP-related photoprotection in each strain. Here, we showed that diverse OCP concentrations could provide the same amplitude of PBS fluorescence quenching in different strains.

Finally, our results suggest that MC does not have a photoprotective role in the studied *Planktothrix* strains: The strain most resistant to light stress does not synthesize MC, and the concentration of MC decreased during light stress in the other two strains.

Author contributions

C.D. did the majority of the immunolocalization work and analyzed data and K.F. realized most of the experiments related to OCP photoprotection and photoinhibition and analyzed data; all the other authors performed experiments and analyzed data; C.B. and D.K. conceived the project, designed and supervised experiments, analyzed data; the article was written by C.B. and D.K. with contributions of S.K.T.

Transparency document

The Transparency document associated with this article can be found, in online version.

Acknowledgements and funding

We thank Dr. Muriel Gugger (Institut Pasteur) for the sequences of the *ocp* and *frp* genes of *Planktothrix* PCC 10110, Dr. Katia Comte (MNHN) for discussion on transcriptomic analysis, Charlotte Duval (MNHN) and Caroline Dalle (Institut Pasteur) for culture of *Planktothrix*. This work was supported by grants from the Agence Nationale de la Recherche (ANR projects CYPHER (ANR-15-CE34-0002-

01)). The research is also supported by the Centre National de la Recherche Scientifique (CNRS, France), the Commissariat à l'Energie Atomique (CEA, France) and the Muséum National d'Histoire Naturelle (MNHN, France). The French Infrastructure for Integrated Structural Biology (FRISBI, France) ANR-10-INBS-05 also partially supported this research. We would like to thank Editage (www.editage.com) for English language editing.

Appendix A. Supplementary data

Supplementary data to this article can be found online at https://doi.org/10.1016/j.bbabio.2019.06.009.

References

[1] K.K. Niyogi, T.B. Truong, Evolution of flexible non-photochemical quenching mechanisms that regulate light harvesting in oxygenic photosynthesis, Curr. Opin. Plant Biol. 16 (2013) 307–314.
[2] C.A. Kerfeld, M.R. Melnicki, M. Sutter, M.A. Dominguez-Martin, Structure, function and evolution of the cyanobacterial orange carotenoid protein and its homologs, New Phytol. 215 (2017) 937–951.
[3] D. Kirilovsky, C.A. Kerfeld, Cyanobacterial photoprotection by the orange carotenoid protein, Nat. Plants 2 (2016) 16180.
[4] N.N. Sluchanko, Y.B. Slonimskiy, E.G. Maksimov, Features of protein-protein interactions in the cyanobacterial photoprotection mechanism, Biochemistry 82 (2017) 1592–1614.
[5] C.A. Kerfeld, M.R. Sawaya, V. Brahmandam, D. Cascio, K.K. Ho, C.C. Trevithick-Sutton, D.W. Krogmann, T.O. Yeates, The crystal structure of a cyanobacterial water-soluble carotenoid binding protein, Structure 11 (2003) 55–65.
[6] C. Punginelli, A. Wilson, J.M. Routaboul, D. Kirilovsky, Influence of zeaxanthin and echinenone binding on the activity of the Orange carotenoid protein, Biochim. Biophys. Acta 1787 (2009) 280–288.
[7] A. Wilson, C. Punginelli, A. Gall, C. Bonetti, M. Alexandre, J.M. Routaboul, C.A. Kerfeld, R. van Grondelle, B. Robert, J.T. Kennis, D. Kirilovsky, A photoactive carotenoid protein acting as light intensity sensor, Proc. Natl. Acad. Sci. U. S. A. 105 (2008) 12075–12080.
[8] C. Bourcier de Carbon, A. Thurotte, A. Wilson, F. Perreau, D. Kirilovsky, Biosynthesis of soluble carotenoid holoproteins in Escherichia coli, Sci. Rep. 5 (2015) 9085.
[9] P.E. Konold, I.H.M. van Stokkum, F. Muzzopappa, A. Wilson, M.L. Groot, D. Kirilovsky, J.T.M. Kennis, Photoactivation mechanism, timing of protein secondary structure dynamics and carotenoid translocation in the orange carotenoid protein, J. Am. Chem. Soc. 141 (2018) 520–530.
[10] R.L. Leverenz, M. Sutter, A. Wilson, S. Gupta, A. Thurotte, C. Bourcier de Carbon, C.J. Petzold, C. Ralston, F. Perreau, D. Kirilovsky, C.A. Kerfeld, PHOTOSYNTHESIS. A 12 a carotenoid translocation in a photoswitch associated with cyanobacterial photoprotection, Science 348 (2015) 1463–1466.
[11] E.G. Maksimov, N.N. Sluchanko, Y.B. Slonimskiy, E.A. Slutskaya, A.V. Stepanov, A.M. Argentova-Stevens, E.A. Shirshin, G.V. Tsoraev, K.E. Klementiev, O.V. Slatinskaya, E.P. Lukashev, T. Friedrich, V.Z. Paschenko, A.B. Rubin, The photocycle of orange carotenoid protein conceals distinct intermediates and asynchronous changes in the carotenoid and protein components, Sci. Rep. 7 (2017) 15548.
[12] S. Gupta, M. Guttman, R.L. Leverenz, K. Zhumadilova, E.G. Pawlowski, C.J. Petzold, K.K. Lee, C.Y. Ralston, C.A. Kerfeld, Local and global structural drivers for the photoactivation of the orange carotenoid protein, Proc. Natl. Acad. Sci. U. S. A. 112 (2015) E5567–E5574.
[13] M. Gwizdala, A. Wilson, D. Kirilovsky, *In vitro* reconstitution of the cyanobacterial photoprotective mechanism mediated by the orange carotenoid protein in *Synechocystis* PCC 6803, Plant Cell 23 (2011) 2631–2643.
[14] D. Harris, O. Tal, D. Jallet, A. Wilson, D. Kirilovsky, N. Adir, Orange carotenoid protein burrows into the phycobilisome to provide photoprotection, Proc. Natl. Acad. Sci. U. S. A. 113 (2016) E1655–E1662.
[15] A. Sedoud, R. Lopez-Igual, A. Ur Rehman, A. Wilson, F. Perreau, C. Boulay, I. Vass, A. Krieger-Liszkay, D. Kirilovsky, The cyanobacterial photoactive orange carotenoid protein is an excellent singlet oxygen quencher, Plant Cell 26 (2014) 1781–1791.
[16] H. Bao, M.R. Melnicki, E.G. Pawlowski, M. Sutter, M. Agostoni, S. Lechno-Yossef, F. Cai, B.L. Montgomery, C.A. Kerfeld, Additional families of orange carotenoid proteins in the photoprotective system of cyanobacteria, Nat. Plants 3 (2017) 17089.
[17] D. Kirilovsky, C.A. Kerfeld, The orange carotenoid protein: a blue-green light photoactive protein, Photochem. Photobiol. Sci. 12 (2013) 1135–1143.
[18] S. Lechno-Yossef, M.R. Melnicki, H. Bao, B.L. Montgomery, C.A. Kerfeld, Synthetic OCP heterodimers are photoactive and recapitulate the fusion of two primitive carotenoproteins in the evolution of cyanobacterial photoprotection, Plant J. 91 (2017) 646–656.
[19] C. Boulay, A. Wilson, S. D'Haene, D. Kirilovsky, Identification of a protein required for recovery of full antenna capacity in OCP-related photoprotective mechanism in cyanobacteria, Proc. Natl. Acad. Sci. U. S. A. 107 (2010) 11620–11625.
[20] M. Gwizdala, A. Wilson, A. Omairi-Nasser, D. Kirilovsky, Characterization of the Synechocystis PCC 6803 fluorescence recovery protein involved in photoprotection, Biochim. Biophys. Acta 1827 (2013) 348–354.
[21] M. Sutter, A. Wilson, R.L. Leverenz, R. Lopez-Igual, A. Thurotte, A.E. Salmeen, D. Kirilovsky, C.A. Kerfeld, Crystal structure of the FRP and identification of the active site for modulation of OCP-mediated photoprotection in cyanobacteria, Proc. Natl. Acad. Sci. U. S. A. 110 (2013) 10022–10027.
[22] A. Wilson, G. Ajlani, J.M. Verbavatz, I. Vass, C.A. Kerfeld, D. Kirilovsky, A soluble carotenoid protein involved in phycobilisome-related energy dissipation in cyanobacteria, Plant Cell 18 (2006) 992–1007.
[23] D. Kirilovsky, R. Kana, O. Prasil, Mechanisms modulating energy arriving at reaction centers in cyanobacteria, in: B. Demmig-Adams, G. Garab, W. Adams, Govindjee (Eds.) Non-Photochemical Quenching and energy dissipation in plants, algae and cyanobacteria, Springer Dordrecht Heidelberg New York London, 2014, pp. 471–501.
[24] J. Huisman, G.A. Codd, H.W. Paerl, B.W. Ibelings, J.M.H. Verspagen, P.M. Visser, Cyanobacterial blooms, Nat. Rev. Microbiol. 16 (2018) 471–483.
[25] E. Dittmann, T. Borner, Genetic contributions to the risk assessment of microcystin in the environment, Toxicol. Appl. Pharmacol. 203 (2005) 192–200.
[26] E. Briand, M. Gugger, J.C. Francois, C. Bernard, J.F. Humbert, C. Quiblier, Temporal variations in the dynamics of potentially microcystin-producing strains in a bloom-forming Planktothrix agardhii (cyanobacterium) population, Appl. Environ. Microbiol. 74 (2008) 3839–3848.
[27] E. Briand, N. Escoffier, C. Straub, M. Sabart, C. Quiblier, J.F. Humbert, Spatiotemporal changes in the genetic diversity of a bloom-forming Microcystis aeruginosa (cyanobacteria) population, ISME J. 3 (2009) 419–429.
[28] C. Tran Du, C. Bernard, M. Ammar, S. Chaouch, K. Comte, Heat shock transcriptional responses in an MC-producing cyanobacterium (Planktothrix agardhii) and its MC-deficient mutant under high light conditions, PLoS One 8 (2013) e73198.
[29] C. Yepremian, M.F. Gugger, E. Briand, A. Catherine, C. Berger, C. Quiblier, C. Bernard, Microcystin ecotypes in a perennial Planktothrix agardhii bloom, Water Res. 41 (2007) 4446–4456.
[30] E. Briand, C. Yepremian, J.F. Humbert, C. Quiblier, Competition between microcystin- and non-microcystin-producing Planktothrix agardhii (cyanobacteria) strains under different environmental conditions, Environ. Microbiol. 10 (2008) 3337–3348.
[31] R. Kurmayer, L. Deng, E. Entfellner, Role of toxic and bioactive secondary metabolites in colonization and bloom formation by filamentous cyanobacteria Planktothrix, Harmful Algae 54 (2016) 69–86.
[32] V. Gaget, M. Welker, R. Rippka, N.T. de Marsac, A polyphasic approach leading to the revision of the genus Planktothrix (cyanobacteria) and its type species, P. agardhii, and proposal for integrating the emended valid botanical taxa, as well as three new species, Planktothrix paucivesiculata sp. nov.ICNP, Planktothrix tepida sp. nov.ICNP, and Planktothrix serta sp. nov.ICNP, as genus and species names with nomenclatural standing under the ICNP, Syst. Appl. Microbiol. 38 (2015) 141–158.
[33] C. Pancrace, M.A. Barny, R. Ueoka, A. Calteau, T. Scalvenzi, J. Pedron, V. Barbe, J. Piel, J.F. Humbert, M. Gugger, Insights into the Planktothrix genus: genomic and metabolic comparison of benthic and planktic strains, Sci. Rep. 7 (2017) 41181.
[34] R.Y. Stanier, R. Kunisawa, M. Mandel, G. Cohen-Bazire, Purification and properties of unicellular blue-green algae (order Chroococcales), Bacteriol. Rev. 35 (1971) 171–205.
[35] A. Catherine, S. Maloufi, R. Congestri, E. Viaggiu, R. Pilkaityte, Cyanobacterial samples: preservation, enumeration, and biovolume measurements, in: J. Meriluoto, L. Spoof, G. Codd (Eds.), Handbook of Cyanobacterial Monitoring and Cyanotoxin Analysis, Wiley, 2017, pp. 333–334.
[36] C. Yéprémian, A. Catherine, R. Congestri, C. Bernard, T. Elersek, R. Pilkaityte, Chlorophyll a extraction and determination, in: J. Meriluoto, L. Spoof, G. Codd (Eds.), Handbook of Cyanobacterial Monitoring and Cyanotoxin Analysis, Wiley, 2017, pp. 315–330.
[37] J. Sun, D. Liu, Geometric models for calculating cell biovolume and surface area for phytoplankton, J. Plankton Res. 25 (2003) 1331–1346.
[38] B. Marie, H. Huet, A. Marie, C. Djediat, S. Puiseux-Dao, A. Catherine, I. Trinchet, M. Edery, Effects of a toxic cyanobacterial bloom (Planktothrix agardhii) on fish: insights from histopathological and quantitative proteomic assessments following the oral exposure of medaka fish (Oryzias latipes), Aquat. Toxicol. 114-115 (2012) 39–48.
[39] Y. Kashino, H. Koike, K. Satoh, An improved sodium dodecyl sulfate-polyacrylamide gel electrophoresis system for the analysis of membrane protein complexes, Electrophoresis 22 (2001) 1004–1007.
[40] K.J. Livak, T.D. Schmittgen, Analysis of relative gene expression data using real-time quantitative PCR and the 2(-Delta Delta C(T)) method, Methods 25 (2001) 402–408.
[41] E.M. Janssen, Cyanobacterial peptides beyond microcystins - a review on co-occurrence, toxicity, and challenges for risk assessment, Water Res. 151 (2019) 488–499.
[42] A. Canini, S. Pellegrini, M. Grilli Caiola, Ultrastructural variations in Microcystis aeruginosa (Chroococcales, Cyanophyta) during a surface bloom induced by high incident light irradiance, Plant Biosyst. 137 (2003) 235–248.
[43] O. Baulina, Ultrastructural Plasticity of Cyanobacteria, Springer-Verlag, Berlin Heidelberg, 2012.
[44] C. Boulay, L. Abasova, C. Six, I. Vass, D. Kirilovsky, Occurrence and function of the orange carotenoid protein in photoprotective mechanisms in various cyanobacteria, Biochim. Biophys. Acta 1777 (2008) 1344–1354.
[45] D. Jallet, A. Thurotte, R.L. Leverenz, F. Perreau, C.A. Kerfeld, D. Kirilovsky, Specificity of the cyanobacterial orange carotenoid protein: influences of orange carotenoid protein and phycobilisome structures, Plant Physiol. 164 (2014) 790–804.
[46] Y. Hihara, A. Kamei, M. Kanehisa, A. Kaplan, M. Ikeuchi, DNA microarray analysis of cyanobacterial gene expression during acclimation to high light, Plant Cell 13 (2001) 793–806.
[47] F.M. Young, C. Thomson, J.S. Metcalf, J.M. Lucocq, G.A. Codd, Immunogold localisation of microcystins in cryosectioned cells of Microcystis, J. Struct. Biol. 151 (2005) 208–214.